3D block modelling of the Sin Quyen IOCG deposit, North Vietnam

Duong Van Hao[1], Nguyen Dinh Chau[2], Wojciech Klityński[3], Władysław Zygo[4], Jakub Nowak[5]

[1] *Vietnam National University, VNU School of Interdisciplinary Studies, Hanoi, Vietnam,*
ORCID ID: 0000-0002-4249-4112
[2] *AGH University of Krakow, Faculty of Geology, Geophysics and Environmental Protection, Krakow, Poland,*
e-mail: cnd@agh.edu.pl (corresponding author), ORCID ID: 0000-0003-1538-6658
[3] *AGH University of Krakow, Faculty of Geology, Geophysics and Environmental Protection, Krakow, Poland,*
ORCID ID: 0000-0001-9852-6665
[4] *AGH University of Krakow, Faculty of Geology, Geophysics and Environmental Protection, Krakow, Poland,*
ORCID ID: 0000-0001-8124-1209
[5] *AGH University of Krakow, Faculty of Physics and Applied Computer Science, Krakow, Poland,*
ORCID ID: 0000-0001-6298-8059

Abstract: The IOCG Sin Quyen deposit is located in the Red River shear zone of North Vietnam. The ore bodies are known as hydrothermal veins and are hosted in Proterozoic metapelite. A block modelling approach was used to build a 3D model of the ore bodies. An analysis was carried out on Surfer® 11 computer software using the archival data recorded from several dozen boreholes distributed within the study area, as well as data obtained from the mineral and chemical analysis of 50 samples collected recently in the deposit. The ore bodies generally trend in a NW-SE direction with an average azimuth of 107° and dip of around 70°. The Cu content in the ore bodies is inhomogeneous. In the bed extension direction, the exponential correlation of Cu concentration in ore bodies is recognized within 2,500 m, while in the direction perpendicular to the bed strike, the exponential dependence is observed on 500 m of distance. The high-grade mineralisation of copper within the ore bodies is often at the altitude interval from ~100 m to ~150 m above sea level (asl). These bodies are also rich in uranium and gold bearing minerals. The total resources of Cu, U and Ag were estimated and amount to 361,000; 12.7 and 11.87 tonnes respectively. The model indicates the downward extension of some ore bodies to below 300 m beneath the ground surface.

Keywords: North Vietnam, iron oxide copper deposits, 3D model, resources, deposit development

INTRODUCTION

The Sin Quyen Cu-Fe deposit is classified as an IOCG type deposit, which are usually characterised by a wide spectrum of polymetallic elements such as: Fe, Cu, Au, Ag, REE and U (Hitzman et al. 1992, Barton & Johnson 2004, Antonenko et al. 2020). There are several well-known deposits of this type in the world, such as the Olympic Dam deposit in South Australia, the Stora Shavaratora and Hannukainen in the Fennoscandian Shield in Sweden, the Dongchuan and the Dahongshan deposit groups or the Qiaoxiahala deposit in China (Hitzman et al. 1992, Weihed et al. 2008, Sandrin et al. 2009, Zhao & Zhou 2011, Li et al. 2014). The ore bodies of IOCG deposits often occur as lenses and dip down near vertically, their resources are from 10 million to above 100 million tonnes of ore with

Cu concentrations ranging from several tenths of a percent to 5%. Most IOCG deposits were formed from magmatic-hydrothermal activity (Sillitoe 2003, Li et al. 2014). IOCG deposits similar to those of the Kiruna type are the end members of a continuum of mineralised systems that typically developed under igneous activity accompanied with high temperature mantle fluid (Hitzman 2000).

Currently, computer science is mostly used in the geosciences for structural models, and 3D geological models are the most effective means of viewing the objects of study and their geological interpretation (Wellmann & Caumon 2018, Gulbin & Mikhalsky 2020, Behera & Sarkar 2021). 3D geological models are also widely used in exploration using various sources of data such as surface geology, boreholes and core holes, seismic, and finally geophysical data including gravimetric and magnetic data (Perin et al. 2005, Wu et al. 2012, Duran et al. 2013, Cheng et al. 2016). 3D models are most effective in the visualisation and correction of maps and plans of ore bodies, ultimately reducing the cost of exploration and mine development. The use of 3D models is not rare in studying the geology of ore deposits, for example 3D models are used to evaluate and enable sometimes to understand the genesis of gold deposits (Liu et al. 2012, Nielsen et al. 2015, Vollgger et al. 2015). 3D modelling has been also carried out to decipher geometrical and geological relationships between breccias, faults and uranium mineralisation zones or the relationships between mineralisation deposits and earlier tectonic processes (Le Carlier de Veslud et al. 2009, Martín-Izard et al. 2015). In active mines, 3D modelling not only allows one to prove the accuracy of the ongoing mining process but also to predict potential mineral targets and to evaluate resources (Gongwen et al. 2001). The methods used for 3D geological models are under continuous development (Sirakov et al. 2001, Lemon & Jones 2003, Calcagno et al. 2008, Maxelon et al. 2009, Gumiel et al. 2010, Wang et al. 2015, Jalloh et al. 2016, Wellmann & Caumon 2018, Kumar 2021).

In the present study, a block model is introduced and defined as an underground cuboid containing the boreholes with known geological and geophysical parameters of the drilled rock layers. To build a 3D geometric model of the ore bodies of the Sin Quyen IOCG deposit, the available previous reported data was analysed together with 50 newly collected samples. The main aims of this study are to:
- determine the geometry and structure of the ore bodies,
- present the spatial distribution of the Cu-U-Ag ore bodies with different grades,
- estimate the ore resource for Cu, Ag, Au, Fe and U,
- predict the potential to extend the ore bodies below 300 m depth.

GEOLOGICAL SETTING

The Sin Quyen IOCG deposit is hosted in the Fanxipan belt in North Vietnam at 22°37′20″ latitude and 103°48′00″ longitude. It is approximately 2 km^2 in area (Ta 1975). The Fanxipan belt belongs to the Ailao Shan-Red River shear zone (ASRR) which is ~1,000 km long, extending from the eastern end of the Himalaya to the west of north Vietnam and stretches up to 300 km long in a NW-SE direction in North Vietnam (Tapponnier et al. 1990, Leloup et al. 1995, McLean 2001, Huang et al. 2013, Pham et al. 2013, Li & Zhou 2018). The ASRR is composed of four metamorphic belts, from NW to SE: Xuelongshan (XLS), Diancangshan (DCS), Fanxipan (FXP) and Day Nui Con Voi (DNCV) (Tapponnier et al. 1990, Calgano et al. 2008, Li & Zhou 2018) (Fig. 1).

The Fanxipan belt is a metamorphic complex including the Suoi Chieng and Sin Quyen formations (Fig. 2). The Suoi Chieng formation, which is nearly 600 m thick, is basically composed of metamorphic rocks such as granitic gneiss, biotite-amphibole gneiss and amphibolite. These rocks were formed from Paleoproterozoic granitoids, terrigenous sediments and mafic volcanic rocks as a consequence of metamorphic processes at 1.97 to 1.83 Ga (Faure et al. 2014, Pham 2015). The Suoi Chieng formation is covered conformably by the Sin Quyen formation which is ~1,200 m thick. From the facies point of view, the Sin Quyen formation is divided into lower and upper units. In the lower unit the prevalent material is graphitic schist, a rock composed of quartz, graphite, muscovite and biotite, while the upper unit is dominated by gneiss principally composed of plagioclase, quartz and biotite.
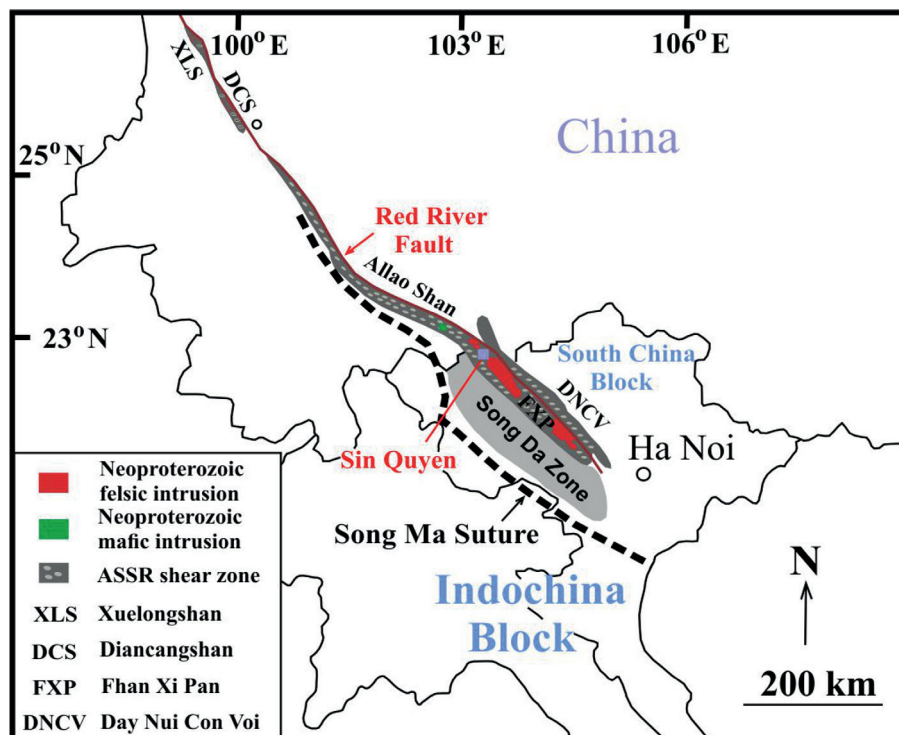
Fig. 1. *Simplified tectonic map of the Ailao Shan-Red River belts in South China and North Vietnam (modified from Li & Zhou 2018)*

The Sin Quyen formation is overlain conformably by the Cam Duong formation built principally from Cambro-Ordovician limestone and marble (McLean 2001, Ishihara et al. 2011, Gas'kov et al. 2012).

The Sin Quyen formation has several Proterozoic and Upper Permian intrusions to earlier Triassic mafic intrusive dikes or lenses. The origin of the intrusive suits is linked to mantle activity Proterozoic intrusive suites of near 1,000 Ma in the Red River zone trending NW-SE were metamorphosed into amphibolites and granitic gneisses (Duong et al. 2021a). These formations occur as lenses and dykes from several metres to a few hundred metres in extent located very close to mineralised zones of the Sin Quyen deposit. Plagioclase (66%), quartz (26%) and biotite (7%) are major components, and microcline, muscovite, sphene, chlorite are minor ones. Ore mineralisation occurred mostly in metamorphic amphibolites, particularly in those places where it is intensely altered. These altered amphibolite zones host approximately 70% of the mineralisation and high-grade zones (McLean 2001). Permian intrusive rocks nearly 250 Ma old present as plagio-granite and occur as small lensoidal bodies of 1 to 20 m width and 100 to 300 m length. Their components are plagioclase, quartz, and biotite (McLean 2001). The mineralising effect of the Permian intrusion is likely to have produced the sulphide mineralisation.

In the Fanxipan belt near the Sin Quyen IOCG deposit there are also Muong Hum HREE, Nam Xe LREE and Dong Pao LREE deposits but, apart from Sin Quyen, none of these are actively mined (Pham et al. 2013).

The Sin Quyen deposit is situated near the boundary between Vietnam and China, trending in a NW-SE direction, near 2,500 m in length and 150 to 500 m in width, and with a depth from a few dozen metres to 600 m (Roger et al. 2012). The deposit area is divided horizontally into two parts NW and SE by the Ngoi Phat stream (Fig. 3).

The first part (1, see Fig. 3) lies predominantly in the western section, where the major minerals in the ore bodies are magnetite, pyrite, chalcopyrite and pyrrhotite contribute from a few percent up to 50% ore composition.
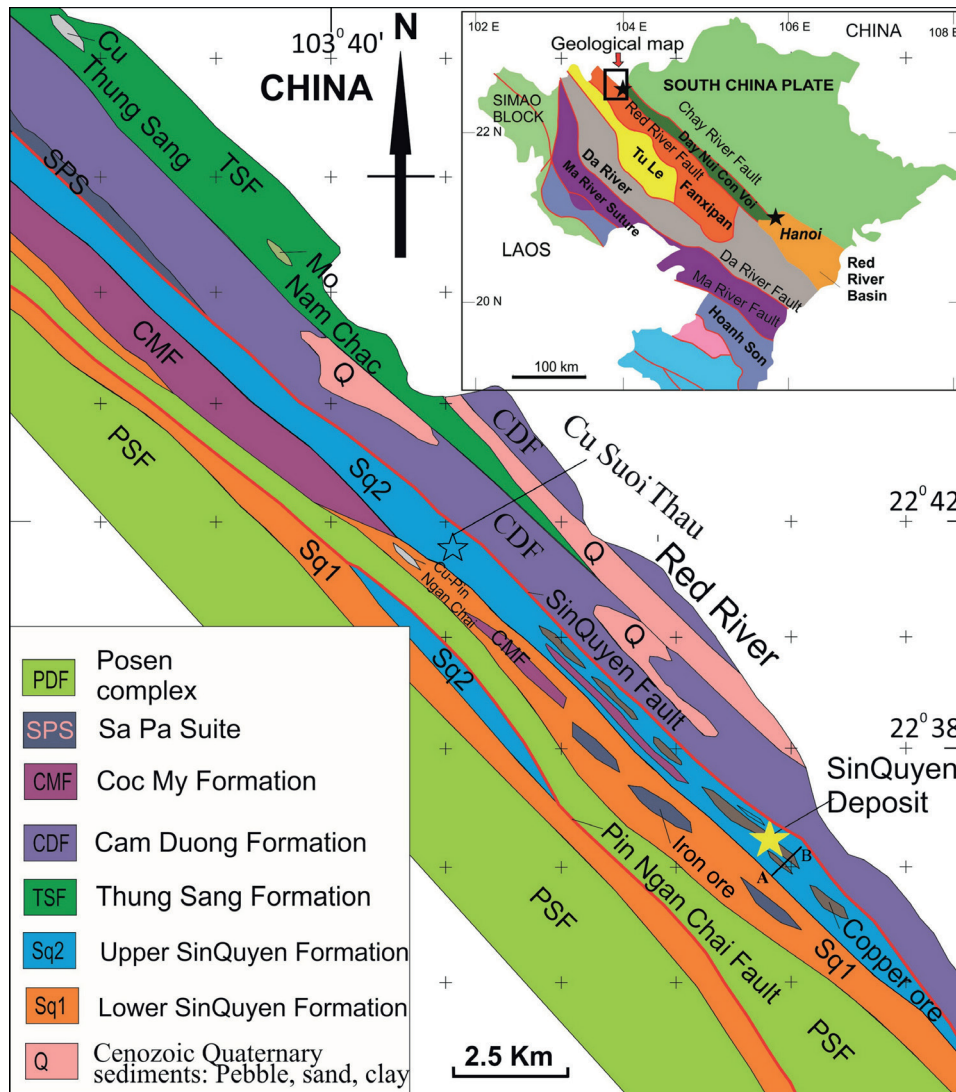
Fig. 2. *The formations occurring in the Fanxipan belt zone on a sketch map of North Vietnam (modified from Duong et al. 2021a)*

The second part (2, see Fig. 3) is widely spread across the central and eastern area, with the main ore minerals in this part being chalcopyrite, pyrrhotite and pyrite, the minerals contributing nearly 90% of the ore composition (McLean 2001, Gas'kov et al. 2012). The ore bodies of the IOCG Sin Quyen deposit are principally hosted in gneiss mica schist in the upper Sin Quyen formation, they occur as breccia lenses several tens of metres thick and up to a few hundred metres long, trending NW-SE with an average azimuth of 110° and dipping nearly vertically (70–90°).

The gneiss is composed of biotite, feldspar and quartz. The mica schist consists of biotite, muscovite, and quartz. The deposit is truncated by two faults. The first is the Sin Quyen reverse fault lying parallel to the Red River fault and trending in a NW direction (Tong-Dzuy et al. 1996, Lepvrier et al. 2008, Liu et al. 2012). The second trends in a NE direction and has a principal role in the forming of the Ngoi Phat stream. The NE fault system represents elements of the South China Blocks which were folded before the Upper Triassic and thrust to the N-NE. In the study deposit the ore occurs as massive, banded, breccia cement and dispersed types. The Cu grade is heterogeneous and often increasing toward the centre of the ore body (Fig. 4). Figure 5 presents a histogram of the Cu concentration, which was prepared on the basis of data from about 500 archival ore samples.
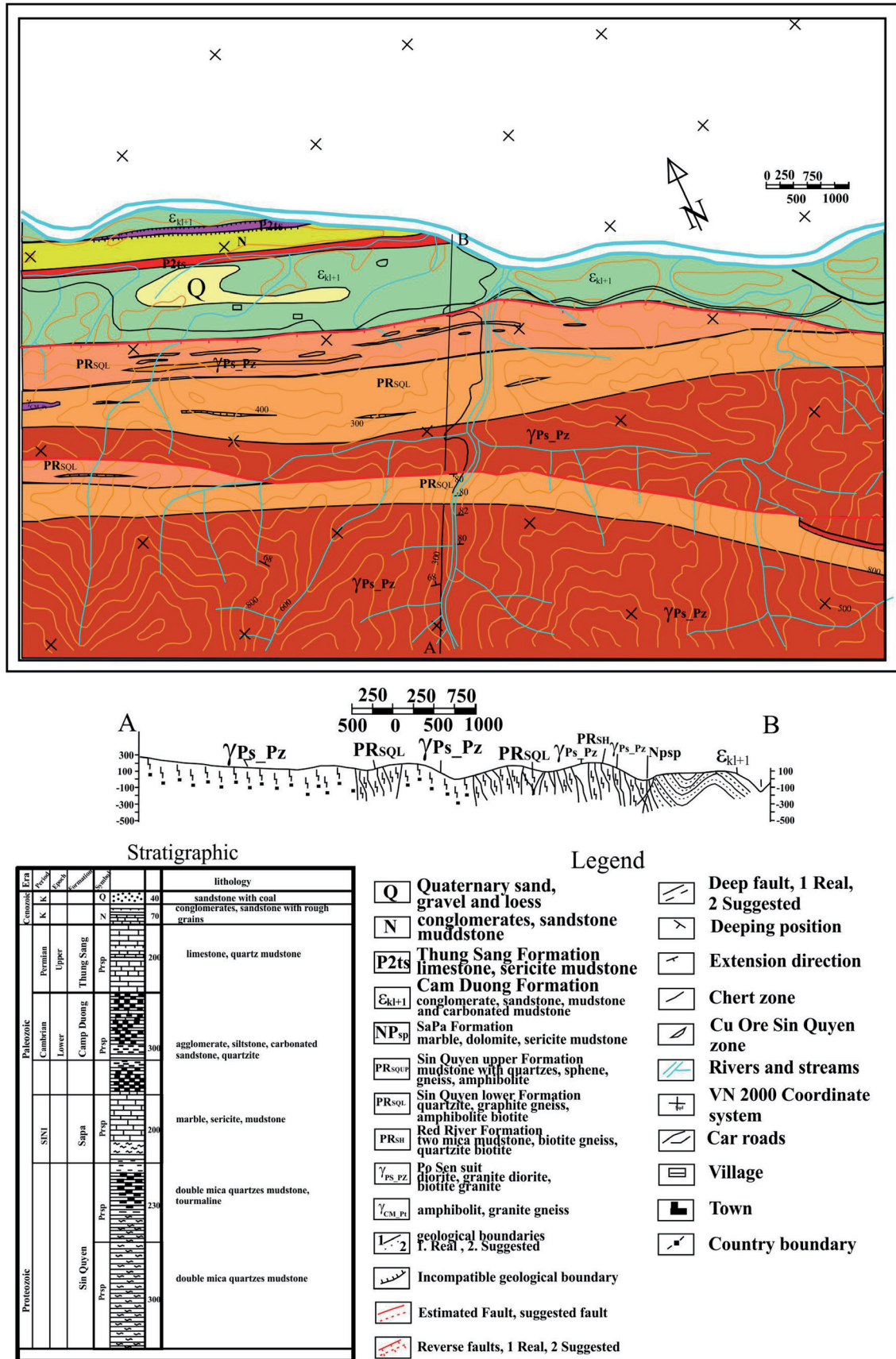
Fig. 3. *A simplified geological map of the IOCG Sin Quyen deposit with geological section AB (modified from Ta 1975)*
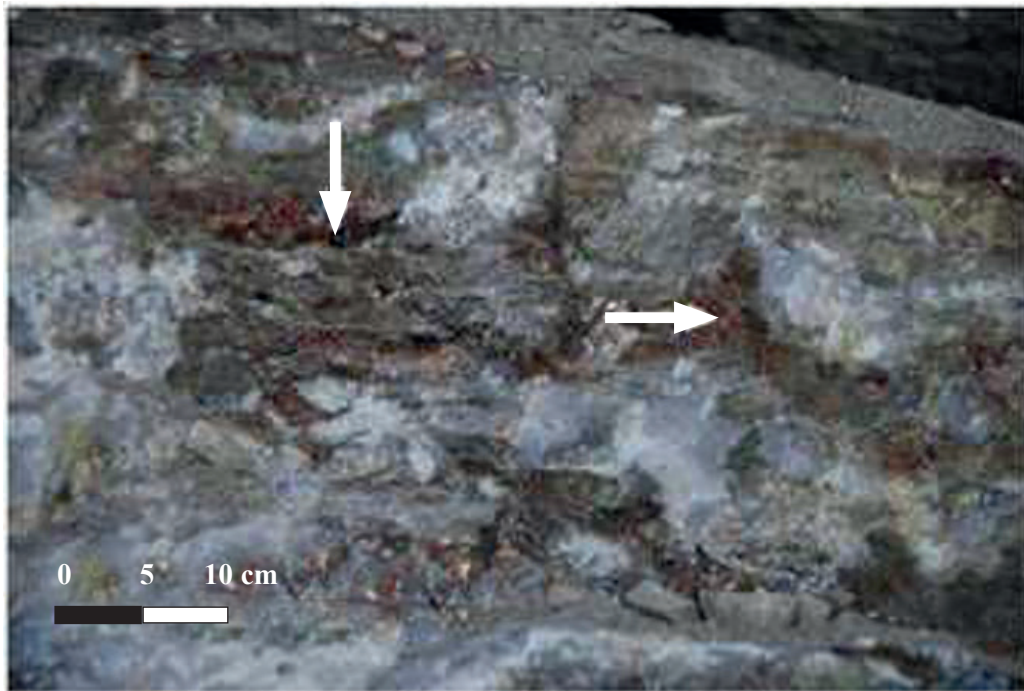
Fig. 4. *An ore body with arrows (→) showing the direction in which the Cu grade increases*
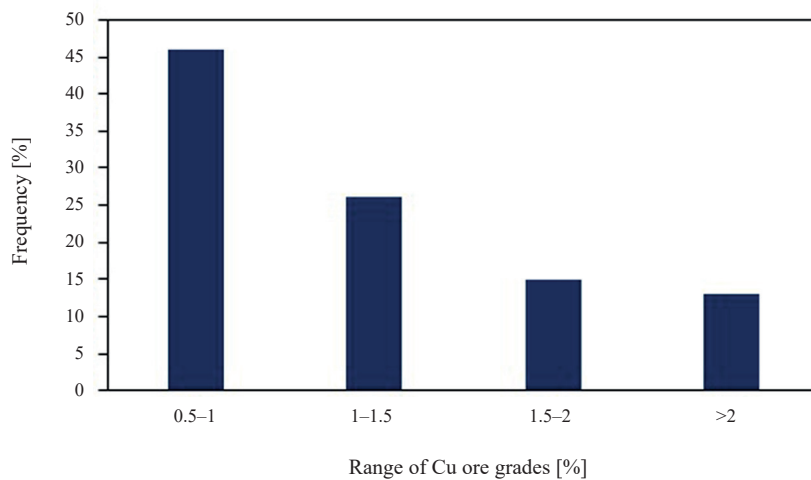

Fig. 5. *Histogram showing the contribution of the Cu grade in 548 ore samples*

The deposit contains about 53 Mt of ore at 22% Fe, 0.9% Cu, 0.7% REE and 0.44 ppm Au on average (McLean 2001, Gas'kov et al. 2012). Since 2016 the Sin Quyen deposit has been exploited as an open pit mine (Fig. 6) with nearly 3,000 Mg Cu concentrate and 1.5 Mg Au as a by-product. Unfortunately to date the REE have not been considered as products, and due to sulphur contamination, the Fe is excluded as uneconomical for commercial production.

Chalcopyrite, pyrite, magnetite, and sphalerite are the major minerals in the deposit, and ilmenite, marcasite, bismuthinite, electrum, native gold, and tellurides are the minor ones (Pieczonka et al. 2019).

Fig. 6. *Photo view of the Sin Quyen IOCG open pit mine (foto A. Piestrzyński)*

THREE-DIMENSIONAL MODELLING

The 3D model enables one to illustrate the distribution of the ore bodies below the surface area, the deposit morphology, and the outcrops of the ore bodies on the surface (Kaufmann & Martin 2008, Wu et al. 2012), but 3D model quality depends on the reliability of the data. In our case, the modelling process is composed of four steps (Fig. 7):

1. input data,
2. computation data,
3. computer modelling,
4. output

In the input we introduced the archival and new data on the deposit area including geological, geophysical and elevation data. The archival data are composed of coordinates, elevation and azimuth of the boreholes, an analysis of the Cu content obtained in the drill cores, gamma intensity and apparent resistivity logging data. The new data are composed of the content of the principal chemical elements Cu, Fe, S and REE analysed in the 50 samples collected from the ore bodies, Cu and Fe concentrates and the flotation reservoir sediment.

In the second step, all of the data were processed in terms of the determination of the statistical parameters and evaluation of the data.

In the third step, the computer has to establish a library with codes for the data, then to build geological cross sections of the ore bodies, in other words to make vertical slide cutting the ore bodies on a given vertical plane.

In the visualisation step all the vertical slides including a morphology map were connected to visualise the 3D model.
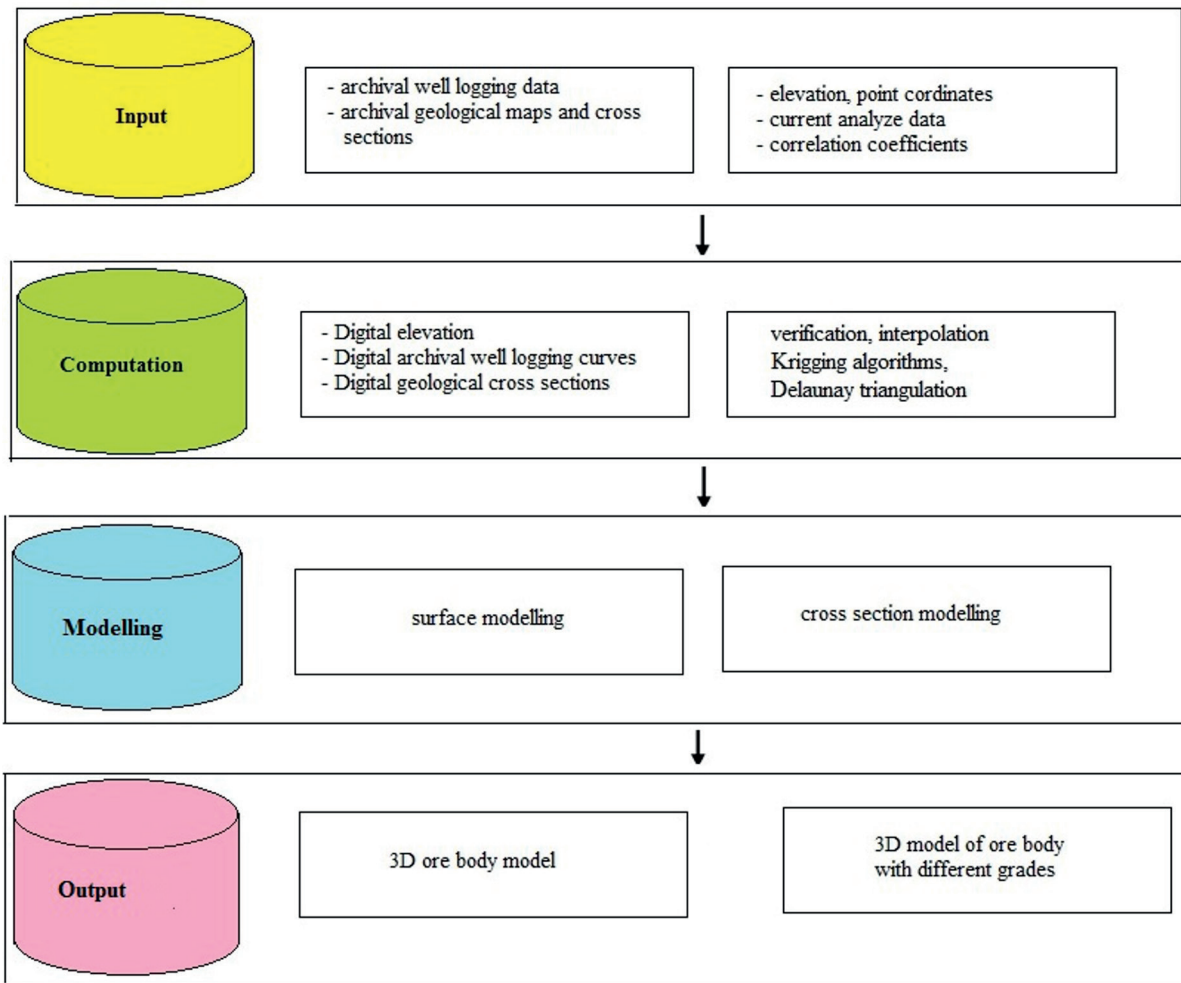
Fig. 7. *Graphic diagram showing the steps in the modelling process*

Input data

A 3D geological model was constructed using archival data as following:

– geographical and geometrical data from the boreholes (coordinate, elevations, depth), azimuth and thickness of the ore bodies drilled;
– data on gamma radiation and apparent resistivity logging, all these archival data were obtained from the Archive Department of the Vietnam General Department of Geology and Mineral Resources;
– concentrations of Cu, Fe, REE and other elements: Si, Al, Ca, Mg, Na, K obtained from the analysis of 50 rock ore samples collected from the study deposit in November 2014.

Processing data

First of all, a block model was constructed incorporating all of the boreholes and ground profiles where geology and geophysics surveys had been performed (Fig. 8).

The block model was divided into nearly 2.4 mln cubes with dimensions of 5 m × 5 m × 5 m, but only the cubes, which are within ore bodies and at their boundaries were considered. As a result of the action, over 200,000 hexahedrons were analysed. The description of every cube in the data file is composed of its geometrical parameters: coordinates, elevation, depth level, azimuth, and angles of dip with trends based on the borehole cores from which the ore body was built up (Fig. 9).
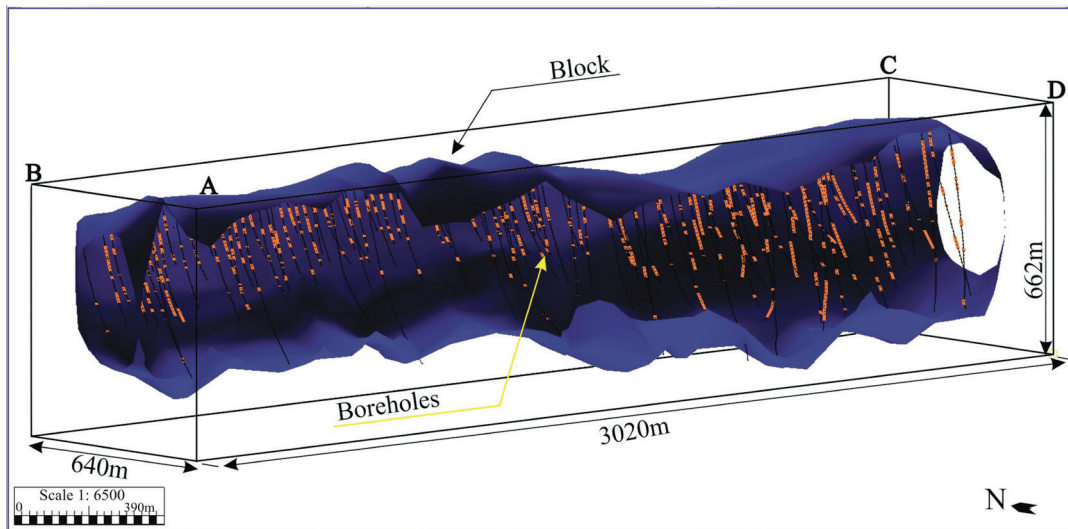
Fig. 8. *The block model*
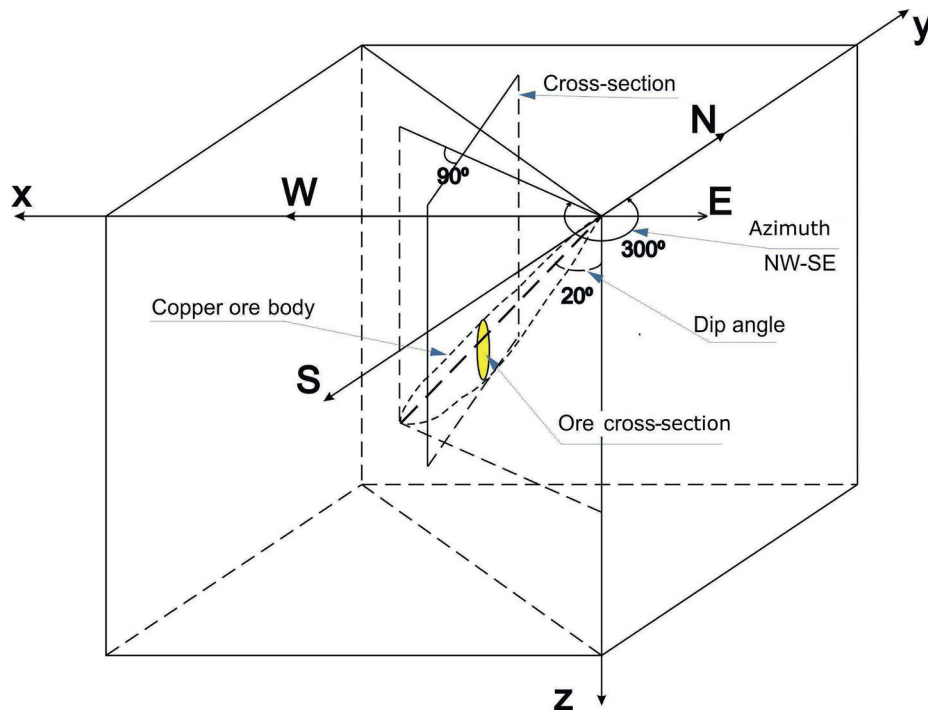
Fig. 9. *The main geometric parameters of the ore body*

Ore body identification based on borehole loggings

The ore bodies were initially identified from the borehole cores. In situations where a core is lacking or the drilled ore bodies identified by geologists are questionable, gamma radiation and apparent resistivity logging data were used (Fig. 10). In Figure 10 the dotted curve presents measures of natural gamma intensity, and the solid curve is one presenting apparent resistivity. There are probably ore bodies in places with high gamma intensity and low apparent resistivity.

Fig. 10. *Determination of a drilled ore body in the IOCG Sin Quyen deposit using the gamma radiation and apparent resistivity borehole logging*

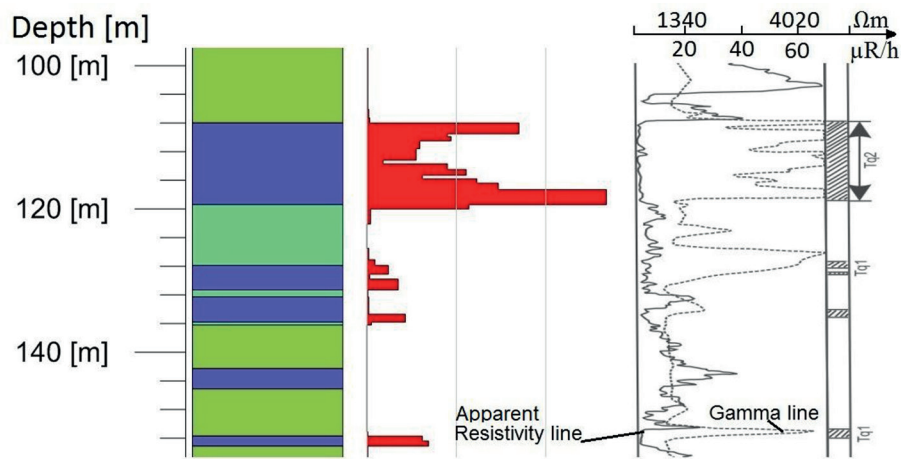## Space variation of Cu concentration in the ore bodies

To track the variability of Cu concentration within ore bodies as a function of distance h, a semivariograms were used. The semivariogram $\gamma_{Cu}(h)$ was calculated as follows:

$$\gamma_{Cu}(h) = \frac{1}{2N(h)} \sum_{i=1}^{N} \left[Cu(z_i + h) - Cu(z_i) \right]^2 \quad (1)$$

where: $N(h)$ is the number of pairs $[Cu(z_i + h) - Cu(z_i)]$ for distance h, z is the distance of sampling in the considered direction.

Based on the archival data of Cu contents from the 980 core samples collected from the 35 boreholes in the deposit area, we chose a depth interval for most of the Cu concentration data which was 70–90 m under surface area. These Cu data of the ore core samples in the mentioned interval were used to create the semivariograms of the Cu concentration in the ore bodies for two directions. The first is the extent direction of the ore bodies (Fig. 11), and the second is the direction perpendicular to the ore bodies strike (Fig. 12).

For the strike of ore bodies, the exponential relation of Cu concentration in the NW-SE is valid on the interval of 2,500 m, while in the NE-SW only on the 500 m of interval with the standard variation of 0.076% and 0.049% respectively. These semivariograms suggest the ore at the given level were probably formed under similar geological conditions. The similar conditions were prevailing on the significantly longer distance on the ore body strike than that on the perpendicular direction.
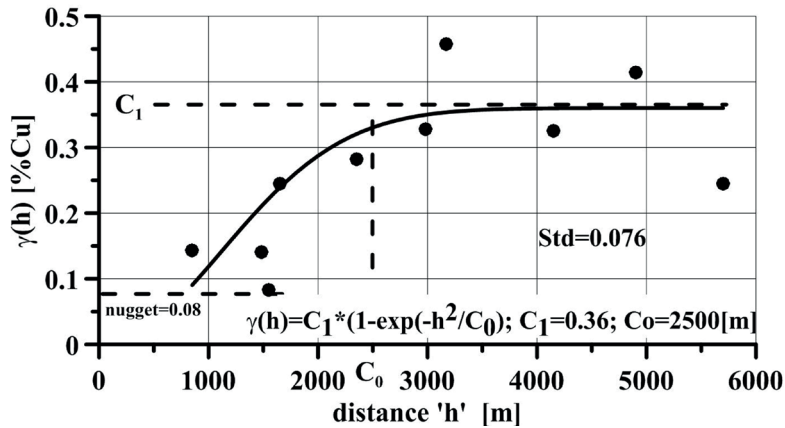

Fig. 11. *Semivariogram of Cu concentration in the extension direction of ore bodies (NW-SE)*
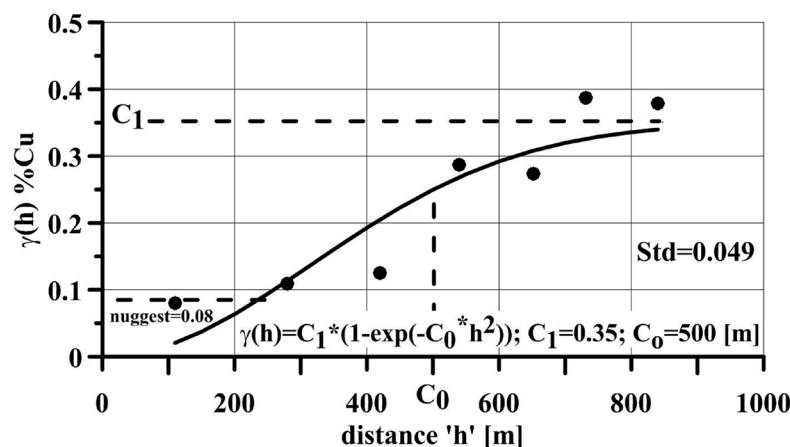
Fig. 12. *Semivariogram of Cu concentration in the direction perpendicular to the extension of ore bodies (NE-SW)*

Determination of the petrophysical parameters

During geological 3D modelling, the attribute model mainly relies on the calculation of the interpolation of data gained by well logging. However, there were some problems observed in the modelling process: the first is connected with the uncertainty of the logging measurement and the second with the estimation of the elements which were not measured directly by well borehole logging methods. Measurements in boreholes are often influenced by different parameters, such as drilling mud, borehole diameter, and the speed of movement of the measuring probes, so the quantitative interpretation is often unsatisfactory. In order to complete the data that is lacking, especially regarding the grades of the elements of interest, the study used linear correlations between Cu, Ag, Au, and U obtained from our previous publication (Duong et al. 2021b). The statistical equations expressing the relations between the concentrations of the mentioned elements are summarized in Table 1.

Table 1
Statistical equations expressing the relation between the grades of the elements Cu, Ag, Au and U in the Sin Quyen ore deposit (Duong et al. 2021b)

Relation	Correlation coefficient R
U(ppm) = 0.0231 Au(ppb) + 46.931	0.78
U(ppm) = 0.086 Ag(ppb) − 13.000	0.81
U(ppm) = 35.457 Cu(%) − 6.025	0.78
Cu(%) = 0.0022 Ag(ppm) + 0.0532	0.94

Interpolation

To show illustrative spatial imaging model for the IOCG Sin Quyen deposit, one needs both geological data, such as azimuth trends and angles of dip of the ore bodies, and the concentrations of the elements concerned (U, Cu, Au, and Ag). In practice, the above-mentioned parameters which describe most of the cubes belonging to the ore body have been interpolated. Interpolation usually relies on geostatistical methods such as kriging, Delaunay triangulation, and discrete smooth interpolation. The kriging algorithm is often used to estimate element concentrations in the spatial elements considered and is primarily based on models presenting the changes of the given parameters as a function of geometrical parameters (angles of azimuth, depth, or distance of ore occurrence). Delaunay triangulation is often used to determine geometrical parameters such as elevation, angle of dip, or the trend of the azimuth. Discrete smooth interpolation (DSI) relies on the estimation of an unknown value of a given parameter for a cube being considered and suppressing uncertainty on the basis of known analytical or statistical functions and the least square method (Stein 1999, Wackernagel 2003, Pham 2015, Liangming et al. 2016). Apart from the mentioned methods, to interpolate data there are also other methods such as minimum curvature and inverse distance weighting. The latter mentioned method was used, since semivariograms were only obtained in the IOCG Sin Quyen deposit at depths of 70–90 m and do not represent the whole deposit.
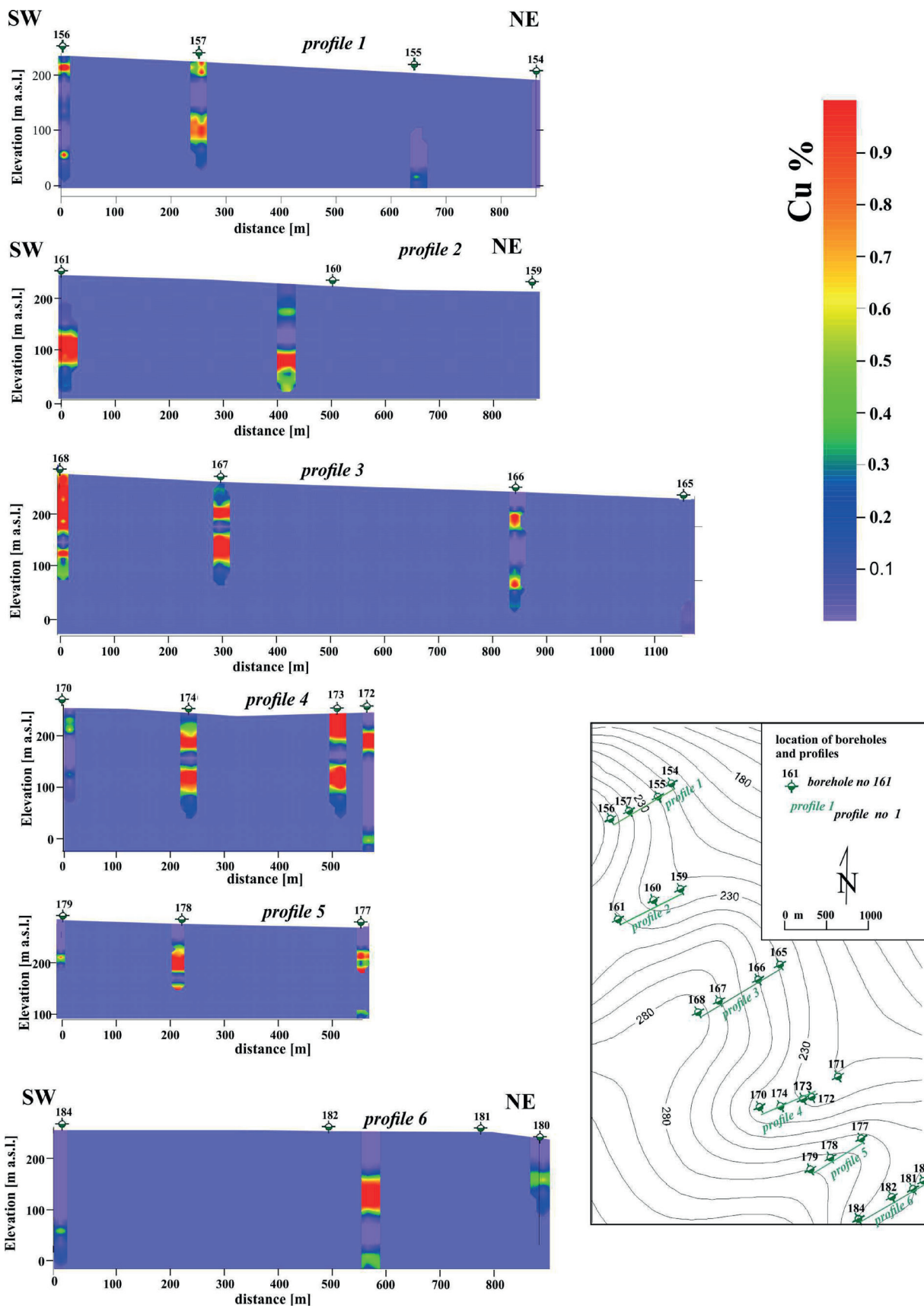
Fig. 13. *Vertical distribution of the Cu content of the selected ore bodies*
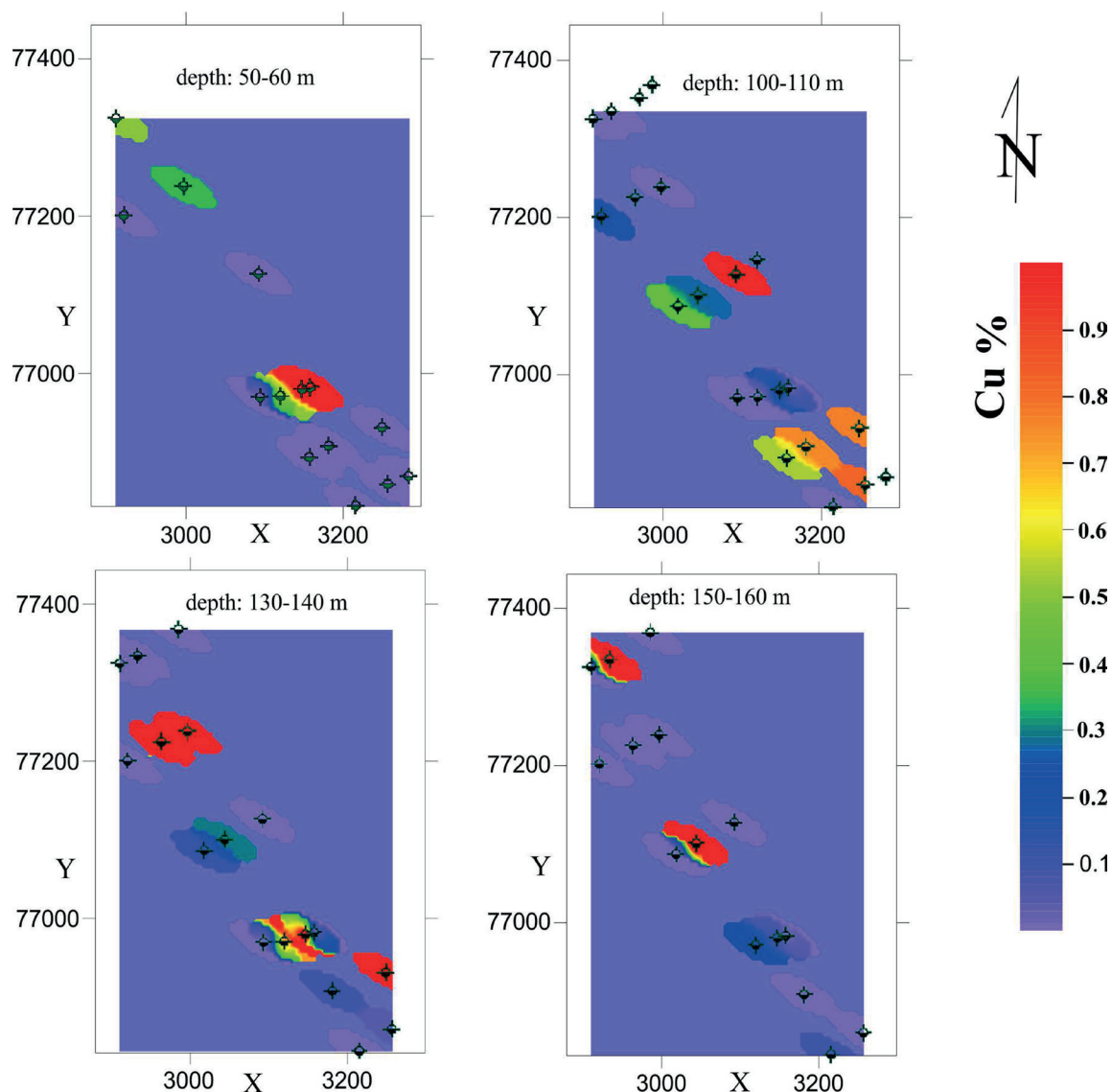
Fig. 14. *Horizontal distribution of the Cu content of the selected ore bodies*

Therefore, we decided to use the inverse distance weighting method to determine the Cu contents and their distribution in the ore bodies in the selected vertical sections is shown on the Figure 13. While the horizontal projections of the ore bodies with the Cu concentration are presented in Figure 14, the extension direction of ore bodies on this figure were made based on the azimuth data of the drilled ore cores. In profiles 4 and 6 of Figure 13, we can see that some ore bodies do not end at a depth of 300 m below the surface, suggesting that some ore bodies might extend further down. The observation was confirmed by a document described by Pham (2015).

THE 3D MODEL

The 3D topography surface model

The 3D topography surface modelling was constructed using a 1:10,000 scale archival topography map of the study deposit as a basic map and the coordinates and elevation of the boreholes within the study area. The digitised elevations at the cross points of a 50 m × 50 m net (5 mm × 5 mm on the map) are stored in a Geodata base. All the morphological data were checked and verified against the elevations of the boreholes within the area (Fig. 15).
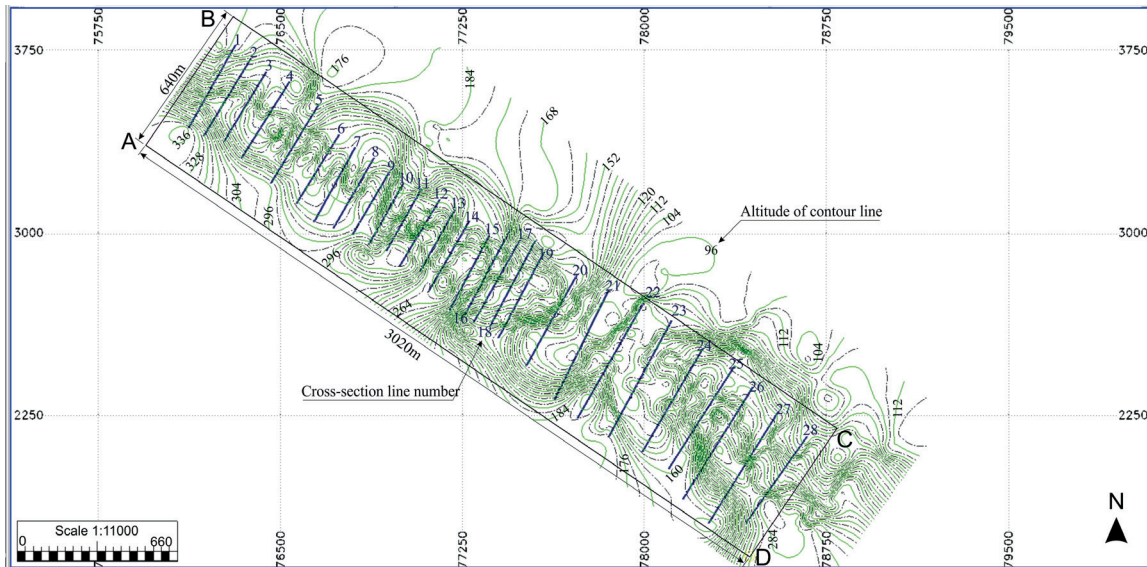
Fig. 15. *Location of the well borehole profiles with the elevation isolines of the deposit area*

The 3D model of the ore bodies

Based on the resulting database, 28 vertical cross-sections were created. In each cross-section the ore body was redrawn in an adequate polygon, which was encoded by a given ID and stored in the system that had been designed (Appendix A). All the ID codes belonging to the same ore body are arranged as a given series and noted on the given row (Appendix A).

The IDs of a given ore body are characterised by their geochemical and geophysical properties, the trend of the azimuth, angle of dip and coordinates of the spatial element belonging to this ore body. The vertical ore cross-section was constructed (Fig. 16) on the basis of the IDs in a given column (profiles 5 and 24). Figure 16 also presents the morphology of the deposit area constructed using the elevation data of the boreholes.
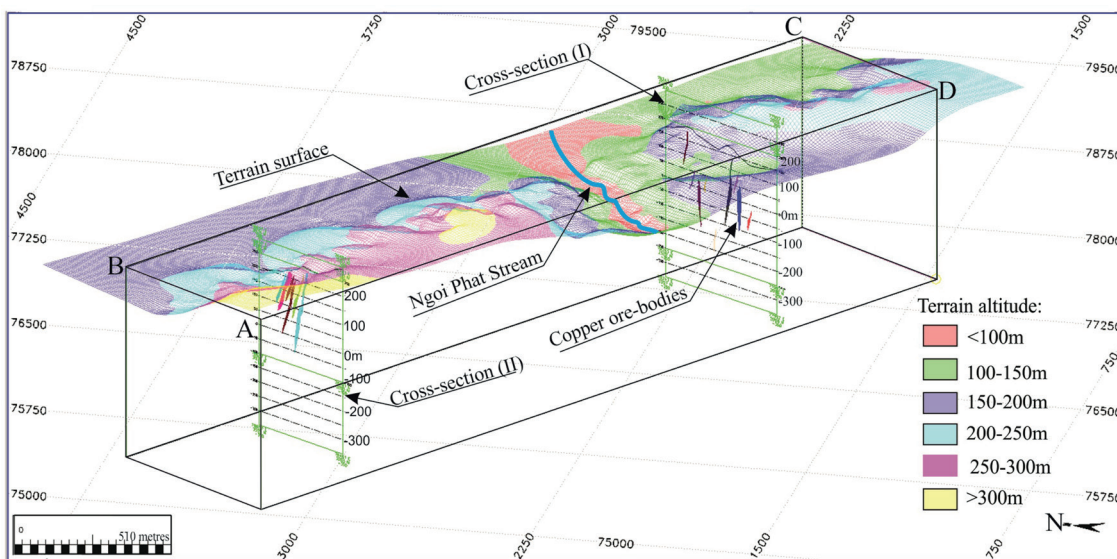
Fig. 16. *Vertical cross sections of ore bodies with the morphology of the modelled area*

The model of the ore body was sketched based on the connections of the IDs belonging to this ore body (Appendix A). Connecting the vertical ore cross sections obtained, the 3D model of the ore bodies was also obtained (Fig. 17). The projections of the ore bodies on the horizontal surface are shown in Figure 18. Based on the distribution of Cu content in the borehole cores, one can calculate ore body models with different grades. For example, Figure 19 presents the model of ore bodies with a Cu grade higher than 0.5%.
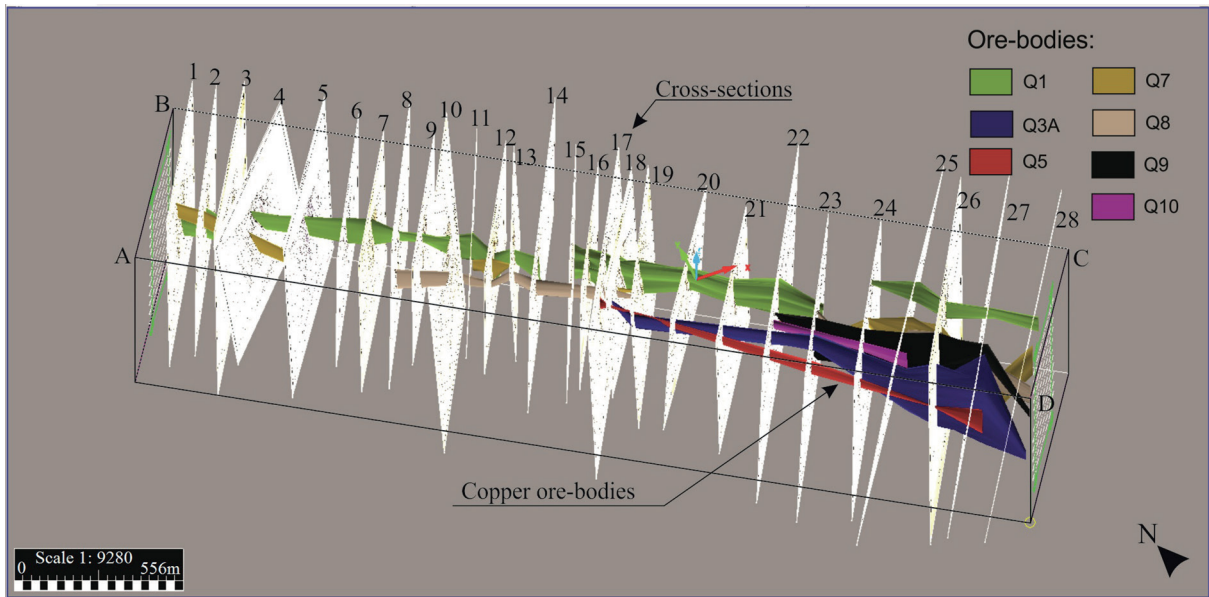
Fig. 17. *3D view of some selected ore bodies on 28 vertical cross sections*
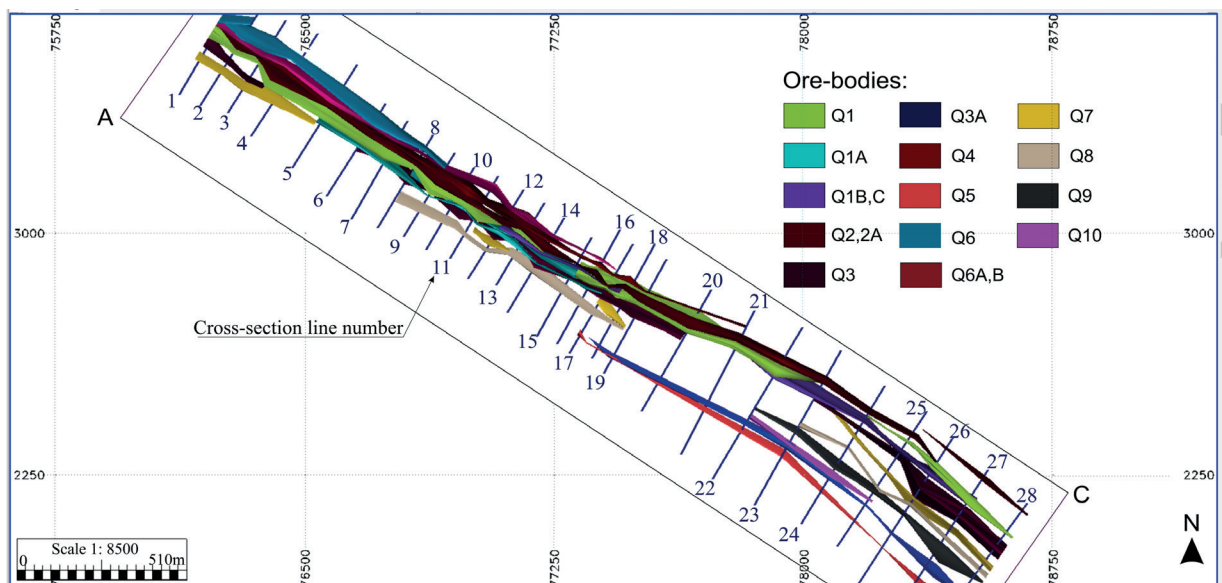
Fig. 18. *Projections of the ore bodies on a horizontal surface*
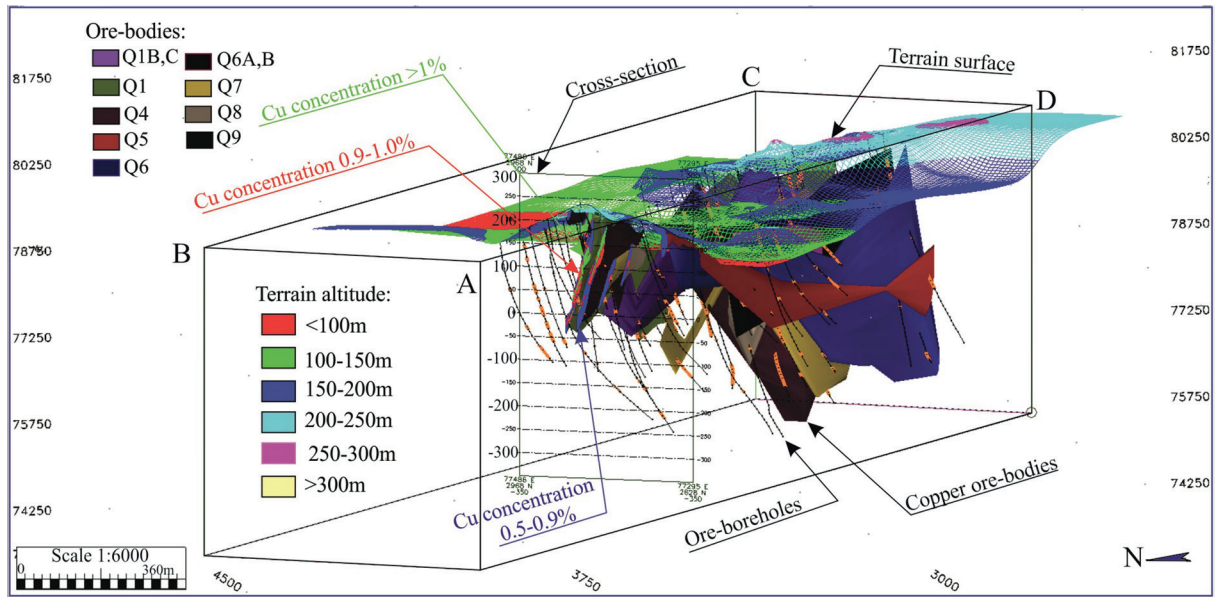
Fig. 19. *Model of the ore bodies with different Cu grades*

Resources

Based on the 3D model and correlations between Cu and the other elements, the resources of Cu, U, Au and Ag in the study deposit were estimated using the relations in Table 1. The calculated volume and Cu resources for each ore body are summarised in Table 2.

Based on the 3D model and reciprocal relations, the copper, uranium and silver resources were estimated as totalling 361,000, 11.9 and 12.7 tonnes respectively (Table 2). The ore bodies with a grade ranging from 0.5 to 1% contribute nearly half of the total resource. The Cu resource, calculated using the 3D model, is nearly 65% of that (550 Gg) published by Ta (1975). The significant difference between the Cu resources might be the consequence of the reasons as follow: (i) during the 1970's, the reserve estimation of the study deposit was based on the data obtained from the documentation of the B category, which was done for the mining project with a standard error that could be ±20% (Nieć et al. 2012); (ii) Ta (1975) might have estimated the Cu resource taking into account ore bodies with a Cu grade far lower than 0.5%. Table 3 also shows "no uranium" in ore bodies with a Cu grade lower than 1.10%, a fact proven by the correlation equation between copper and uranium (Table 1).

Table 2
Calculated Cu, Ag and U resources

Name of ore body	Volume [× 1,000 m³]	Density [kg/m³]	Mass of ore [Gg]	Average Cu grade [%]	Cu mass [Gg]	Ag amount [kg]	U amount [kg]
Q1	3,610	3,210	1,160	1.16	13.4	580	4,030
Q1a	908	3,170	2,880	1.23	35.4	1,540	2,160
Q1b, c	1,340	3,210	4,297	1.11	47.7	2,060	2,480
Q2, 2a	1,510	3,300	5,000	1.19	59.4	2,580	2,600
Q3	5,280	3,270	1,730	1.03	17.8	770	–
Q3a	391	3,040	1,190	1.31	15.6	680	1,450
Q4	957	3,200	3,060	0.88	26.9	1,200	–
Q5	899	3,104	2,820	0.68	19.2	80	–

Table 2 cont.

Q6	497	3,120	1,550	0.62	9.62	40	–
Q6a, b	1,250	3,000	3,740	0.90	33.6	1,430	–
Q7	1,130	3,000	3,400	0.71	24.1	1,020	–
Q8	670	3,000	2,010	0.90	18.1	770	–
Q9	1,370	3,000	4,120	0.90	37.0	1,580	–
Q10	119	3,150	374	0.76	2.84	120	–
Sum	19,931	–	37,331	–	361	11,870	12,720

DISCUSSION

The paper presents a methodology for using different types of accessible geophysical data and geological and geographical information (geological maps, well borehole data, geochemical data, cross-sections, morphology) to construct a 3D geological model with the help of the Surfer® 11 software. The methodology relies on the structuring and storing of geological digital data. The reliable archival and new data were verified and validated based on the geological and mining information obtained, as well as using geostatistical methods. The main data used were geological, such as geometrical parameters and concentrations of the analysed elements of the ore body cores obtained during the drilling of holes. The well geophysics logging data were used to identify the geological lithology of the drilled beds and the ore bodies in the boreholes, as well as in the case of lack of the cores. The geostatistical methods enable us to track the behaviour of the Cu concentrations parallel and perpendicular to the bodies' extension. The Cu concentration values of the ore samples in the parallel ore bodies are significantly better correlated than that of the samples in the direction perpendicular to the body extension. This fact is probably related to (i) the similarity of the geochemical properties of the whole elements in the ore body and (ii) the ore body forming process could mostly be related to the local conditions. The 3D model of the Sin Quyen IOCG deposit was built using the 3D topography surface model and 3D block. The 3D topography surface model was constructed based on the coordinates and elevations of the boreholes and the localization of the main natural objects such as the Ngoi Phap Stream. Due to the net of the geological boreholes, the topography surface model presents the original deposit area, which affects the variability of the Cu, Fe and other elements in the deposit, especially the zone near the ground surface, since a tropical climate predominates. The 3D topography could help to back up the original topographic conditions for use in geological studies. In this application, the bodies of Cu ore were modelled as volumes composed of special cube elements located within the Sin Quyen IOCG deposit. The geometrical framework can serve to estimate the volume of the Cu ore bodies, which were used to calculate the resources of the metals of interest.

The 3D block of the ore bodies was constructed based on both the geometrical ore bodies (trend of azimuth, angle of dip, thickness, and length) and the connecting of all the vertical cross sections modelled using the ID codes of the ore bodies. The ID codes contain the data of an ore body elevation, trend of azimuth, thickness, and angle as well as the Cu contents. Thanks to the data of the ID codes, one could connect the given elements to the ore body present in the different vertical cross sections. Both the archival and current analysed Cu concentration data of the ore samples enabled us to build the 3D model of the ore bodies with different Cu levels and the Cu resources were also estimated. The new calculated resources with different Cu concentrations are a clear success of the 3D modelling in comparison with the older geological methods used in the 1970's. The difference of the former calculated Cu resource and current one could be related to the archival data of the class C1, which could be related deviation up to 30% (Ta 1975, Nieć et al. 2012). Due to the good correlations between Cu concentrations and the U, Au and Ag ones, the resources of uranium, gold and silver were also appreciated. In the study deposit, the unclear correlation between Cu and REE might be a consequence of the different

periods of the ores bearing the mentioned elements (Pieczonka et al. 2019).

The combination of data sets and geological information for reserve assessment can face many difficulties. Therefore, the modelling employed is essential, as well as the requisite computer software. Assessment in this approach can be better and cheaper for calculating, evaluating and predicting the reserves and potential of ore bodies which will continuously extend downward from the explored levels. It can be seen that the ore bodies have continuously extended downward to the northeast and the near surface in the southwest of study area. The results also show the reserves and space shape for each of the ore bodies, which will useful in calculating reserves as well as the further exploitation of each ore body and the whole mine.

CONCLUSIONS

The IOCG Sing Quyen deposit has been very interesting for geologists from different fields, from those determining the presence of different useful elements to those focused on its resources since the 1960's, when the deposit was discovered during the geomagnetic and radiometry and geological cartography prospecting works. Although the area of this deposit is not large ~2 km^2, as well as the main elements (Cu, Fe) in it, there are also precious sources of REE, Ag, Au, and radioactive elements (U). The deposit is also interesting from the structural and origin point of view. Generally, the deposit consists of two parts with different dominating minerals and their origin is related to the tectonic processes which formed the Ailao Shan-Red River shear zone, which happened in different geological periods from Neoproterozoic up to Kenozoic.

The authors of this work attempted to present the space model of the ore bodies based mainly on both the archival geological and geophysics data and the current analysed data of the collected samples. The 3D model could be significantly improved if the large mass of geological and geophysical data that was lost during the border war between China and Vietnam that took place in 1979 were to be found again. In places where data is sparse or not credible, the use of geostatistical algorithms was necessary to determine the parameters of the bodies. However, the semivariograms show the similarity of the geological conditions prevailing at a 70–90 m depth interval. The 3D model also allows us to calculate the Cu, Ag and U resources. The Cu resource calculated using the 3D model differs significantly from that estimated in the 1970's. Based on the 3D model, we can state that the minerals containing Ag and Au (mainly electrum in the study deposit) can be distributed within the ore body, on the other hand minerals containing U (mainly uraninite) can mostly be observed in the body zone with high grades of Cu.

In our opinion, this methodology can be developed and applied for the investigation of other ore deposits in which not only the ore bodies but also sedimentary and intrusive formations can be visualised. The 3D deposit model could constitute a useful role in the study of the origin and history of how a deposit developed in the past. In this case, the geological formations and the relationship between the different geological suits and regional and local geodynamic information should be defined in detail. This methodology can also be applied to the modelling of ore bodies lying over deposits of any metal ores that originate from hydrothermal origins or for other deposits where ore bodies occur in different forms.

REFERENCES

Antonenko A.A., Zhukov N.M., Pavlova Z.N. & Gikolova T.V., 2020. The Varvarinskoye complex copper-gold deposit in Northern Kazakhstan: Mineral types and ore composition. *Geology of Ore Deposits*, 62, 314–331. https://doi.org/10.1134/S1075701520030022.

Barton M.D. & Johnson D.A., 2004. Footprints of Fe-oxide (-Cu-Au) system. [in:] Knox-Robinson C.M. (ed.), *SEG 2004: Predictive Mineral Discovery Under Cover: Extended Abstracts*, Centre for Global Metallogeny, the University of Western Australia Publication, 33, The University of Western Australia, Perth, Western Australia, 112–116.

Behera S.G. & Sarkar B.C., 2021. Geostastical modelling and vertical effect analysis of a Ferruginous East Coast bauxite deposit, India. *Geology of Ore Deposits*, 63, 269–285. https://doi.org/10.1134/S1075701521030028.

Calcagno P., Courrioux G., Guillen A. & Chiles J.P., 2008. Geological modelling from field data and geological knowledge. Part I. modelling method coupling 3D potential field interpolation and geological rules. *Physics of the Earth and Planetary Interiors*, 171, 147–157. https://doi.org/10.1016/j.pepi.2008.06.013.

Cheng F., Liu J., Wang J., Zong Y. & Yu M., 2016. Multi-hole seismic modeling in 3-D space and cross-hole seismic tomography analysis for boulder detection. *Journal of Applied Geophysics*, 134, 246–252. https://doi.org/10.1016/j.jappgeo.2016.09.014.

Duong V.H., Trinh P.T., Thanh N.D., Piestrzynski A., Nguyen D.C., Pieczonka J., Dac N.X. et al., 2021a. Cu-Au mineralization of the Sin Quyen deposit in north Vietnam: A product of Cenozoic left-lateral movement along the Red River shear zone. *Ore Geology Reviews*, 132, 104065. https://doi.org/10.1016/j.oregeorev.2021.104065.

Duong V.H., Nguyen D.C., Piestrzyński A. & Pieczonka J., 2021b. Relationship between selected major, minor, and trace elements in iron oxide–copper–gold deposits, an example from the unique Sin Quyen Deposit (Lào Cai Province, North Vietnam). *Russian Geology & Geophysics*, 62(11), 1214–1228. https://doi.org/10.2113/RGG20194156

Duran E.R., di Primio R., Anka Z., Stoddart D. & Horsfield B., 2013. 3D-basin modelling of the Hammerfest Basin (southwestern Barents Sea): A quantitative assessment of petroleum generation, migration and leakage. *Marine and Petroleum Geology*, 45, 281–303. https://doi.org/10.1016/j.marpetgeo.2013.04.023.

Faure M., Lepvrier C., Nguyen V.V., Vu T.V., Lin W. & Chen Z., 2014. The South China block-Indochina collision: Where, when, and how? *Journal of Asian Earth Sciences*, 79(A), 260–274. https://doi.org/10.1016/j.jseaes.2013.09.022.

Gas'kov I.V., Tuan-Anh T., Hoa T.T., Thi Dung P., Nevol'ko P.A. & Ngoc Can P., 2012. The Sin Quyen Cu-Fe-Au-REE deposit (northern Vietnam): composition and formation conditions. *Russian Geology and Geophysics*, 53(5), 442–456. https://doi.org/10.1016/j.rgg.2012.03.005.

Gongwen W., Shouting Z., Changhai Y., Yaowu S., Yue S., Dong L. & Fengming X., 2011. Mineral potential targeting and resource assessment based on 3D geological modeling in Luanchuan region, China. *Computers & Geosciences*, 37(12), 1976–1988. https://doi.org/10.1016/j.cageo.2011.05.007.

Gulbin Y.L. & Mikhalsky E.V., 2020. Modeling of mineral parageneses and thermobarometry of metavolcanic rocks of the Ruker Group in the Southern Prince Charles Mountains, East Antarctica. *Geology of Ore Deposits*, 62(7), 584–598. https://doi.org/10.1134/S1075701520070053.

Gumiel P., Arias M. & Martín-Izard A., 2010. 3D geological modelling of a polyphase deformed pre-Variscan IOCG mineralization located at the southeastern border of the Ossa Morena Zone, Iberian Massif (Spain). *Geological Journal*, 45(5–6), 623–633. https://doi.org/10.1002/gj.1192.

Hitzman M.W., 2000. Iron oxide-Cu-Au deposits: what, where, when, and why. [in:] Porter, T.M. (ed.), *Hydrothermal Iron Oxide Copper-Gold & Related Deposits: A Global Perspective. Vol. 1*, PGC Publishing, Adelaide, 9–25.

Hitzman M.W., Oreskes N. & Einaudi M.T., 1992. Geological characteristics and tectonic setting of Proterozoic iron oxide (Cu-U-Au-REE) deposits. [in:] Gaál G. & Schulz K. (eds.), *Precambrian Metallogeny Related to Plate Tectonics*, Precambrian Research, 58(1–4), Elsevier Science Publishers, Amsterdam, Netherlands, 241–287. https://doi.org/10.1016/0301-9268(92)90121-4.

Huang H.H., Xu Z.J., Wu Y.M., Song X., Huang B.S. & Nguyen L.M., 2013. First local seismic tomography for Red River shear zone, northern Vietnam: Stepwise Kriging employing crustal P and Pn waves. *Tectonophysics*, 584, 230–239. https://doi.org/10.1016/j.tecto.2012.03.030.

Ishihara S., Hirano H., Hoshino M., Ngoc Can P., Thi Dung P. & Tuan-Anh T., 2011. Mineralogical and chemical characteristics of the allanite-rich Cu and iron ores from the Sin Quyen mine, northern Vietnam. *Bulletin of the Geological Survey of Japan*, 62(5–6), 197–209. https://doi.org/10.9795/bullgsj.62.197.

Jalloh A.B., Sasaki K., Jalloh Y. & Barrie A.K., 2016. Integrating artificial neural networks and geostatistics for optimum 3D geological block modelling in mineral reserve estimation: A case study. *International Journal of Mining Science and Technology*, 26(4), 581–585. https://doi.org/10.1016/j.ijmst.2016.05.008.

Kaufmann O. & Martin T., 2008. 3D geological modelling from boreholes, cross-sections and geological maps, application over former natural gas storages in coal mines. *Computers & Geosciences*, 34(3), 278–290. https://doi.org/10.1016/j.cageo.2007.09.005.

Kuma A. & Dimitrakopoulos R., 2022. Updating geostatistically simulated models of mineral deposits in real-time with incoming new information using actor-critic reinforcement learning. *Computers & Geosciences*, 158, 104962. https://doi.org/10.1016/j.cageo.2021.104962.

Le Carlier de Veslud C., Cuney M., Lorilleux G., Royer J.J. & Jébrak M., 2009. 3D modelling of uranium-bearing-solution collapse breccias in Proterozoic sandstones (Athabasca basin, Canada) Metallogenic interpretations. *Computers & Geosciences*, 35(1), 92–107. https://doi.org/10.1016/j.cageo.2007.09.008.

Leloup P.H., Lacassin R., Tapponnier P., Schärer U., Zhong D., Liu X., Zhang L. et al., 1995. The Ailao Shan-Red River shear zone (Yunnan, China), Tertiary transform boundary of Indochina. *Tectonophysics*, 251(1–4), 13–84. https://doi.org/10.1016/0040-1951(95)00070-4.

Lemon A.M. & Jones N.L., 2003. Building solid models from boreholes and user-defined cross-sections. *Computers & Geosciences*, 29(5), 547–555. https://doi.org/10.1016/S0098-3004(03)00051-7.

Lepvrier C., Van Vuong N., Maluski H., Truong Thi P. & Van Vu T., 2008. Indosinian tectonics in Vietnam. *Comtes Redus Geoscience*, 340(2–3), 94–111. https://doi.org/10.1016/j.crte.2007.10.005.

Li Q., Zhang Z., Geng X., Li C., Liu F., Chai F. & Yang F., 2014. Geology and Geochemistry of the Qiaoxiahala Fe-Cu-Au deposit, Junggar region, northwest China. *Ore Geology Reviews*, 57, 462–481. https://doi.org/10.1016/j.oregeorev.2013.08.003.

Li X.C. & Zhou M.F., 2018. The nature and origin of hydrothermal REE mineralization in the Sin Quyen deposit, Northwestern Vietnam. *Economic Geology*, 113(3), 645–673. https://doi.org/10.5382/econgeo.2018.4565.

Liangming L., Jianfeng L., Ruichao Z. & Tao S., 2016. 3D modeling of the porphyry-related Dawangding gold deposit in south China: Implications for ore genesis and resources evaluation. *Journal for Environmental and Economic Geochemistry*, 164, 164–185. https://doi.org/10.1016/j.gexplo.2015.11.002.

Liu J., Tran M.D., Tang Y., Nguyen Q.L., Tran T.H., Wu W., Chen J. et al., 2012. Permo-Triassic granitoids in the northern part of the Truong Son belt, NW Vietnam: Geochronology, geochemistry and tectonic implications. *Gondwana Research*, 122(2), 628–644. https://doi.org/10.1016/j.gr.2011.10.011.

Mallet J.L., 1997. Discrete modeling for natural objects. *Mathematical Geology*, 29, 199–219. https://doi.org/10.1007/BF02769628.

Martín-Izard A., Arias D., Arias M., Gumiel P., Sanderson D.J., Castañon C., Lavandeira A. & Sanchez J., 2015. A new 3D geological model and interpretation of structural evolution of the world-class Rio Tinto VSM deposit, Iberian Pyrite Belt (Spain). *Ore Geology Reviews*, 71, 457–476. https://doi.org/10.1016/j.oregeorev.2015.06.006.

Maxelon M., Renard P., Courrioux G., Brändli M. & Mancktelow N., 2009. A workflow to facilitate three-dimensional geometrical modelling of complex poly-deformed geological units. *Computers & Geosciences*, 35(3), 644–658. https://doi.org/10.1016/j.cageo.2008.06.005.

McLean R.N., 2001. The Sin Quyen iron oxide-Cu-gold-rare earth oxide mineralisation of North Vietnam. [in:] Porter T.M. (ed.), *Hydrothermal Iron Oxide Copper-Gold & Related Deposits: A Global Perspective. Vol. 2*, PGC Publishing, Adelaide, 293–301.

Nieć M., Mucha J., Sobczyk E. & Wasilewska-Błaszczyk M., 2012. *Metodyka dokumentowania złóż kopalin stałych. Część IV: Szacowanie zasobów* [*Methodology of geological reporting of mineral deposits. Pt. 4, Resource estimation*]. Wydawnictwo IGSMiE PAN, Kraków.

Nielsen S.H., Cunningham F., Hay R., Partington G. & Stokes M., 2015. 3D protectivity modelling of orogenic gold in the Marymia Inlier, Western Australia. *Ore Geology Review*, 71, 578–591. https://doi.org/10.1016/j.oregeorev.2015.02.001.

Perin M., Zhu B., Rainaud J.-F. & Schneider S., 2005. Knowledge-driven application for geological modelling. *Journal of Petroleum Science and Engineering*, 47(1–2), 89–104. https://doi.org/10.1016/j.petrol.2004.11.010.

Pham T.H., 2015a. *The geological characteristics and copper potential reserve below 150 m deep level at the Sin Quyen Copper deposit, Lao Cai province, Northwestern Vietnam*. UMG, Hanoi [MSc thesis, in Vietnamese].

Pham T.H., 2015b. The Ngoi Chi Formation in Fan Si Pan area of Northwest Vietnam revealed by zircon U-Pb age and Hf isotope composition. *Acta Geoscientica Sinica*, 36(6), 755–760. https://doi.org/10.3975/cagsb.2015.06.07

Pham T.H., Chen F.K., Thuy N.T.B., Cuong N.Q. & Li S.Q., 2013. Geochemistry and zircon U–Pb ages and Hf isotopic composition of Permian alkali granitoids of the Phan Si Pan zone in northwest Vietnam. *Journal of Geodynamics*, 69, 106–121. https://doi.org/10.1016/j.jog.2012.03.002.

Pieczonka J., Nguyen C.D., Piestrzyński A. & Le P.K., 2019. Timing of ore mineralization using ore mineralogy and U-Pb dating, Iron Ox ide Cop per Gold Sin Quyen de posit, North Vietnam. *Geological Quarterly*, 63(4), 861–874. https://doi.org/10.7306/gq.1507.

Roger F., Maluski H., Lepvrier C., Vu Van T. & Paquette J.L., 2012. LA-ICPMS zircon U/Pb dating of Permo-Triassic and Cretaceous magmatisms in Northern Vietnam – Geodynamical implications. *Journal of Asian Earth Sciences*, 49, 72–82. https://doi.org/10.1016/j.jseaes.2011.12.012.

Sandrin A., Edfelt A., Waight T.E., Berggren R. & Elming S.-A., 2009. Physical properties and petrologic description of rock samples from an IOCG mineralized area in the northern Fennoscandian Shield, Sweden. *Journal of Geochemical Exploration*, 103(2–3), 80–96. https://doi.org/10.1016/j.gexplo.2009.07.002.

Sillitoe R.H., 2003. Iron oxide-copper-gold deposits: an Adrean view. *Mineralium Deposita*, 38, 787–812. https://doi.org/10.1007/s00126-003-0379-7.

Sirakov N.M. & Muge F.H., 2001. A system for reconstructing and visualising 3D objects. *Computers & Geosciences*, 27(1), 59–69. https://doi.org/10.1016/S0098-3004(00)00055-8.

Stein M.L., 1999. *Interpolation of Spatial Data: Some Theory for Kriging*. Springer, New York.

Ta V.D., 1975. *Report of geological surveys and their results performed at the IOCG Sin Quyen deposit in Lao Cai, North Vietnam*. Main Department of Geology of Vietnam [in Vietnamese].

Tapponnier P., Lacassin R., Leloup P.H., Schärer U., Dalai Z., Haiwei W. & Xiaohan L., 1990. The Ailao Shan/Red River metamorphic belt: Tertiary left-lateral shear between Indochina and South China. *Nature*, 343, 431–437. https://doi.org/10.1038/343431a0.

Tong-Dzuy T., Janvier P. & Ta H.P., 1996. Fish suggest continental connections between the Indochina and South China blocks in Middle Devonian time. *Geology*, 24(6), 571–574. https://doi.org/10.1130/0091-7613(1996)024<0571:FSCCBT>2.3.CO;2.

Vollgger S.A., Cruden A.R., Ailleres L. & Cowan E.J., 2015. Regional dome evolution and its control on ore-grade distribution: Insights from 3D implicit modelling of the Navachab gold deposit, Namibia. *Ore Geology Reviews*, 69, 268–284. https://doi.org/10.1016/j.oregeorev.2015.02.020

Wackernagel H., 2003. *Multivariate Geostatistics: An Introduction with Applications*. Springer, Berlin, Heidelberg.

Wang G., Zhang S., Yan C., Song Y., Sun Y., Li D. & Xu F., 2015. 3D geological modeling for prediction of subsurface Mo targets in the Luanchuan district, China. *Ore Geology Reviews*, 71, 592–610. https://doi.org/10.1016/j.oregeorev.2015.03.002.

Weihed P., Eilu P., Larsen R.B., Stendal H. & Tontti M., 2008. Metallic mineral deposits in the Nordic countries. *Episodes*, 31(1), 125–132. https://doi.org/10.18814/epiiugs/2008/v31i1/017.

Wellmann F. & Caumon G., 2018. 3-D Structural Geological Models: Concepts, Methods, and Uncertainties. *Advances in Geophysics*, 59, 1–121. https://doi.org/10.1016/bs.agph.2018.09.001.

Wu J., Sun Y., Wang B., Wang Y., Xu L. & Dai C., 2012. 3D geological modeling of fractured volcanic reservoir bodies in Block DX18 in Junggar Basin, NW China. *Petroleum Exploration and Development*, 39(1), 99–106. https://doi.org/10.1016/S1876-3804(12)60020-2.

Zhao X.F. & Zhou M.F., 2011. Fe-Cu deposits in the Kangdian region, SW China: a Proterozoic IOCG (iron-oxide-copper-gold) metallogenic province. *Mineralium Deposita*, 46, 731–747. https://doi.org/10.1007/s00126-011-0342-y.

APPENDIX A

Ore bodies and their ID code in different vertical cross-sections

Ore body	Profile number													
	1	**2**	**3**	**4**	**5**	**6**	**7**	**8**	**9**	**10**	**11**	**12**	**13**	**14**
Q1	23	57	64	74	88	101	113	132	142	159	165	178	188	201
Q1a	–	–	–	–	93	100	112	124	91	157	164	179	173	198
Q1b	–	–	–	–	92	103	121	73	141	156	163	180	186	491
Q1c	24	56		75	89	107	118	116	135	158	–	–	–	–
Q2	25	58	69	77	87	106	117	85	143	161	169	110	190	202
Q2a	–	59	–	–	–	–	111	–	–	–	–	–	–	–
Q3	–	55	65	79	72	104	122	90	140	96	168	125	174	128
Q3a	50	47	48	–	–	–	–	–	–	–	–	–	–	–
Q4	61	–	71	78	86	102	114	127	94	149	170	175	192	203
Q5	–	–	–	–	84	103	115	126	95	150	123	–	193	130
Q6	–	–	–	–	–	–	–	–	–	–	–	–	194	204
Q6a	–	–	–	–	–	–	–	–	–	–	–	–	–	–
Q6b	–	–	–	–	–	–	–	–	–	–	–	–	–	–
Q7	–	–	66	80	97	–	–	–	138	153	166	–	–	–
Q8	–	–	67	81	98	–	–	129	139	154	167	184	–	199
Q9	–	–	–	–	–	–	–	–	–	–	–	–	–	–
Q10	–	–	–	–	–	–	–	–	–	–	–	–	–	–
Ore body	**Profile number**													
	15	**16**	**17**	**18**	**19**	**20**	**21**	**22**	**23**	**24**	**25**	**26**	**27**	**28**
Q1	213	219	225	282	244	131	271	281	298	303	324	338	356	343
Q1a	–	220	264	–	–	–	–	148	–	–	–	–	–	–
Q1b	–	–	–	–	–	–	–	136	–	305	263	337	144	–
Q1c	–	–	–	–	–	–	–	–	–	–	–	–	–	–
Q2	212	218	229	134	245	261	–	283	297	304	325	340	–	–
Q2a	–	–	–	–	–	–	–	–	–	–	–	–	–	–
Q3	214	216		240	243	265	270	–	292	–	318	334	145	342
Q3a	–	–	–	–	–	–	–	–	–	–	–	–	–	–
Q4	211	133	230	235	247	260	272	–	–	–	–	–	–	–
Q5	210	70	492	207	248	259	273	–	–	–	–	–	–	–
Q6	209	215	233	208	249	258	274	–	–	–	–	–	–	–
Q6a	–	–	–	–	–	256	275	–	–	–	–	–	–	–
Q6b	–	–	–	–	–	257	–	–	–	–	–	–	–	–
Q7	–	–	222	241	242	266	269	285	299	307	316	332	365	146
Q8	–	–	–	–	–	–	–	–	291	306	315	330	–	346
Q9	–	–	221	–	–	–	268	278	290	302	314	329	137	345
Q10	–	–	–	–	–	–	–	277	–	301	312	–	–	–